required to quantify such an effect; if it were shown to be important, however, it could have implications for ozone mitigation strategies.

The variability of $\gamma(N_2O_5)$ with aerosol composition has potential impacts on other issues. They include the export of NO_x from the boundary layer to the free troposphere, the global burden of oxidants such as O_3 and OH (*10*), and the seasonal variations in NO_x and related chemistry. Our results point toward such influences, but additional in situ measurements of NO_x, NO_3, N_2O_5, O_3, VOC, and aerosol from aircraft and other platforms in different locations and seasons will be required to address these questions.

References and Notes

1. P. J. Crutzen, *Annu. Rev. Earth Planet. Sci.* **7**, 443 (1979).
2. R. P. Wayne *et al.*, *Atmos. Environ.* **25A**, 1 (1991).
3. U. Platt, F. Heintz, *Isr. J. Chem.* **34**, 289 (1994).
4. A. M. Winer, R. Atkinson, J. N. J. Pitts, *Science* **224**, 156 (1984).
5. S. S. Brown *et al.*, *Geophys. Res. Lett.* **31**, 10.1029/2004GL019412 (2004).
6. Materials and methods can be found on *Science* Online.
7. M. J. Evans, D. J. Jacob, *Geophys. Res. Lett.* **32**, 10.1029/2005GL022469 (2005).
8. N. Riemer *et al.*, *J. Geophys. Res.* **108**, 10.1029/2002JD002436 (2003).
9. X. Tie, G. Brasseur, L. Emmons, L. Horowitz, D. Kinnison, *J. Geophys. Res.* **106**, 22931 (2001).
10. F. J. Dentener, P. J. Crutzen, *J. Geophys. Res.* **98**, 7149 (1993).
11. U. F. Platt, A. M. Winer, H. W. Bierman, R. Atkinson, J. N. Pitts Jr., *Environ. Sci. Technol.* **18**, 365 (1984).
12. S. S. Brown, H. Stark, A. R. Ravishankara, *J. Geophys. Res.* **108**, 10.1029/2003JD003407 (2003).
13. E. R. Lovejoy, D. R. Hanson, *J. Phys. Chem.* **99**, 2080 (1995).
14. M. Hallquist, D. J. Stewart, S. K. Stephenson, R. A. Cox, *Phys. Chem. Chem. Phys.* **5**, 3453 (2003).
15. M. Hallquist, D. J. Stewart, J. Baker, R. A. Cox, *J. Phys. Chem. A* **104**, 3984 (2000).
16. S. M. Kane, F. Caloz, M.-T. Leu, *J. Phys. Chem. A* **105**, 6465 (2001).
17. J. H. Hu, J. P. D. Abbatt, *J. Phys. Chem. A* **101**, 871 (1997).
18. A. Wahner, T. F. Mentel, M. Sohn, *Geophys. Res. Lett.* **25**, 2169 (1998).
19. A. Stohl, M. Hittenberger, G. Wotawa, *Atmos. Environ.* **32**, 4245 (1998).
20. J. A. Thornton, C. F. Braban, J. P. Abbatt, *Phys. Chem. Chem. Phys.* **5**, 4593 (2003).
21. M. Folkers, T. F. Mentel, A. Wahner, *Geophys. Res. Lett.* **30**, 10.1029/2003GL017168 (2003).
22. J. A. Thornton, J. P. D. Abbatt, *J. Phys. Chem.* **109**, 10004 (2005).
23. D. M. Murphy, *Science* **307**, 1888 (2005).
24. T. F. Mentel, M. Sohn, A. Wahner, *Phys. Chem. Chem. Phys.* **1**, 5451 (1999).
25. C. F. Braban, J. P. D. Abbatt, *Atmos. Chem. Phys.* **4**, 1451 (2004).
26. R. Atkinson, J. Arey, *Chem. Rev.* **103**, 4605 (2003).
27. R. G. Derwent, M. E. Jenkin, S. M. Saunders, M. J. Pilling, *J. Air Waste Manage. Assoc.* **51**, 699 (2001).
28. M. Mozurkewich, J. G. Calvert, *J. Geophys. Res.* **93**, 15889 (1988).

29. We thank E. Atlas and S. Donnelly for VOC data from canister samples, which was supported by both NOAA and NSF, and the crew of the NOAA P-3 aircraft. This work was supported by NOAA's Health of the Atmosphere and Climate and Global Change Programs. R.W. gratefully acknowledges the financial support of NOAA through contract NA04OAR4310089.

Supporting Online Material

www.sciencemag.org/cgi/content/full/311/5757/67/DC1
Materials and Methods
SOM Text
Figs. S1 to S3
References

13 September 2005; accepted 18 November 2005
10.1126/science.1120120

An Unusual Marine Crocodyliform from the Jurassic-Cretaceous Boundary of Patagonia

Zulma Gasparini,[1]* Diego Pol,[2] Luis A. Spalletti[3]

Remains of the marine crocodyliform *Dakosaurus andiniensis* from western South America reveal a lineage that drastically deviated from the skull morphology that characterizes marine crocodyliforms. The snout and lower jaw are extremely robust, short, and high and only bear a few large teeth with serrated edges (resembling those of some terrestrial carnivorous archosaurs). This unusual morphology contrasts with the long and gracile snout and lower jaws bearing numerous teeth, which are present in the closest relatives of *D. andiniensis* (and interpreted as indicating feeding on small fish or mollusks). Thus, the morphological diversity of pelagic marine crocodyliforms was wider than had been thought.

The fossil record of Crocodyliformes (crocodiles and extinct relatives) shows a wide morphological and ecological diversity. One of the most remarkable examples is Thalattosuchia, the only group of archosaurs completely adapted to the marine environment (*1*). This group is characterized by numerous features, including an extremely long and tubular hyperdentate snout (*1*, *2*). Here we describe a fossil crocodyliform from Patagonia that further expands this variation.

[1]Consejo Nacional Investigaciones Científicas y Técnicas (CONICET), Departamento de Paleontología de Vertebrados, Facultad de Ciencias Naturales y Museo, Universidad Nacional de La Plata, Paseo del Bosque s/n, 1900 La Plata, Argentina. [2]Mathematical Biosciences Institute, The Ohio State University, 231 West 18th Avenue, Columbus, OH 43210, USA. [3]CONICET, Centro de Investigaciones Geológicas, Facultad de Ciencias Naturales y Museo, Universidad Nacional de La Plata, Calle 1, 644, 1900 La Plata, Argentina.

*To whom correspondence should be addressed. E-mail: zgaspari@museo.fcnym.unlp.edu.ar

In the Southern Hemisphere, most Mesozoic marine crocodyliforms have come from the Vaca Muerta Formation (*3*–*5*) in the Neuquén Basin (western Argentina; fig. S1). An extremely fragmentary crocodyliform specimen was previously discovered in this unit and named *Dakosaurus andiniensis* (*6*) because of some similarities with *D. maximus* (*7*) from the Jurassic in Europe. However, the fragmentary nature of this enigmatic material offered few answers about the habits and relationships of this large marine crocodyliform.

Two new specimens of *D. andiniensis* were recently found in Pampa Tril (fig. S1)—a rich, fossiliferous locality of the Vaca Muerta Formation—and are referred to this taxon because of the presence of autapomorphic characters for a marine crocodyliform (*8*). One of these includes a lower jaw (specimen identification: MOZ 6140P), and the other (MOZ 6146P) consists of an almost-complete skull and lower jaws (Fig. 1 and fig. S2). The new skull is almost complete and reveals an unusual skull and dental morphology. The skull and mandible are approximately 80 cm long from the anterior end to the cranio-mandibular articulation. The snout is high with respect to its anteroposterior length (Fig. 1 and fig. S2), compared with all other marine crocodyliforms (*2*–*9*), and measures 42 cm long and 15.3 cm high (measured at the anteroposterior midpoint of the rostrum). The lateromedial width of the rostrum is subequal to its dorsoventral depth. Anteriorly, the rostrum tapers rapidly, producing an unusual bullet-shaped skull. Most of the dorsal surface of the snout is convex and level with the dorsal surface of the frontal and supratemporal region. The subcircular orbit faces laterally and is large, constituting approximately 18% of the skull length. A large scleral ring is preserved in this opening. The elongated antorbital fossa is obliquely oriented, and the lacrimal, nasal, maxilla, and jugal bones form its margins, as in metriorhynchid thalattosuchians (*2*–*10*).

The premaxilla is only preserved on the left side and encloses a large narial opening, although the dorsomedial region of this element is unknown for this taxon. The maxilla is notably short and high and extends dorsally, contacting its counterpart and separating the nasals from the premaxilla. This element contributes to 65% of the rostral length. The nasals are short and broad, but they project posteroventrally as a long and acute process onto the lateral surface of the snout. The lacrimals are only exposed on the lateral surface of the rostrum and are dorsally sutured to the extensive prefrontal and nasals. The enlarged prefrontal extends onto the lateral surface of the snout and overhangs the orbit, a synapomorphic character of metriorhynchids (*2*).

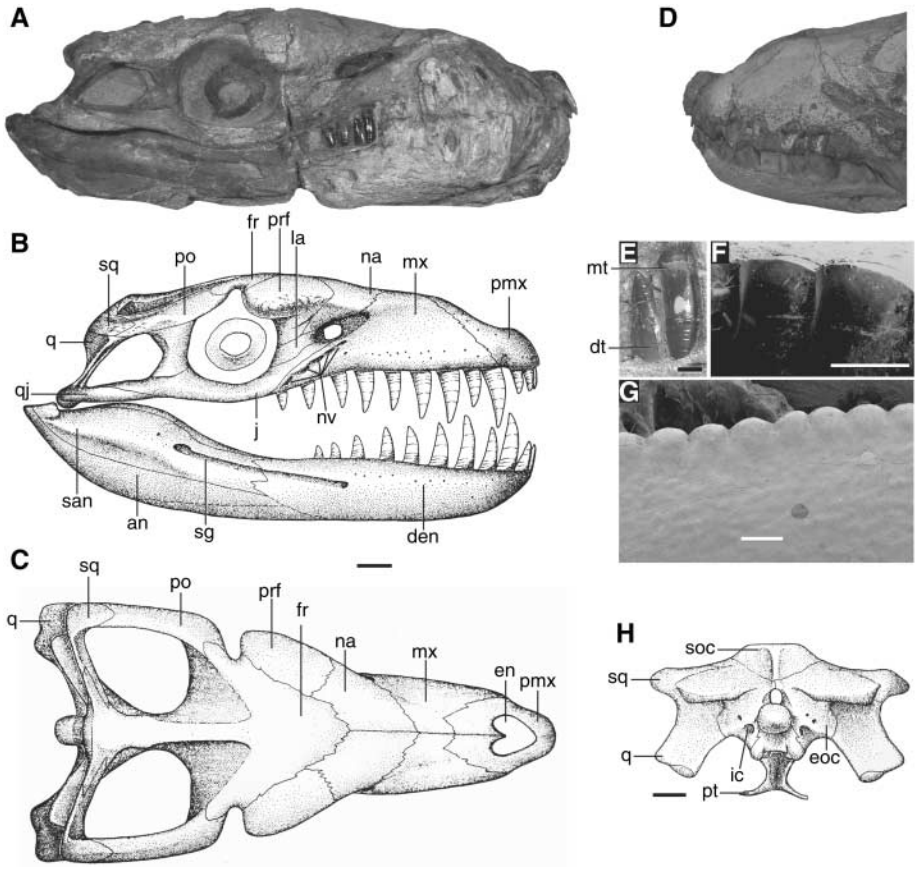

Fig. 1. *D. andiniensis* MOZ 6146P in (**A**) right lateral view. Skull reconstruction in lateral (**B**), dorsal (**C**), and occipital (**H**) views (based on left and right sides). (**D**) Rostrum in left dorsolateral view. (**E**) Posterior maxillary and dentary teeth. (**F** and **G**) Mesial denticles in mesial (F) and buccal (G) views. Scale bars, 5 cm [(A) to (D) and (H)]; 5 mm, (E); and 500 μm [(F) and (G)]. Abbreviations: an, angular; den, dentary; dt, dentary tooth; en, external nares; eoc, exoccipital; fr, frontal; ic, internal carotid foramen; la, lacrimal; mt, maxillary tooth; mx, maxilla; na, nasal; nv, neurovascular foramina; pmx, premaxilla; po, postorbital; prf, prefrontal; pt, pterygoid; q, quadrate; qj, quadratojugal; san, surangular; sg, surangular groove; soc, supraoccipital; sq, squamosal.

The frontals and parietals are completely fused into single elements, as in all mesoeucrocodylians (*10*). The straight frontal-nasal suture runs at a 45° angle with the sagittal plane, resembling the condition of *D. maximus* (*7*). The squamosal has a short anterior branch, and the postorbital extends ventrally on the lateral surface of the postorbital bar, continuous with the lateral surface of the jugal as in all thalattosuchians (*10*). The quadrate is well developed, with robust articular condyles, and it contacts the ventrolateral flange of the exoccipital as in all crocodyliforms (*10*). The basioccipital is low and bears small basioccipital tubera, contrasting with the developed condition of marine crocodyliforms. The exoccipital bears a large foramen for the internal carotid artery on its ventrolateral flange. The palatines form an extended secondary palate and enclose with pterygoids a wide choanal opening.

The mandible is high, robust, and slightly diverges posteriorly, following the narrow outline of the skull, which contrasts with the low and gracile morphology of other marine crocodyliforms (*1*, *2*, *11*). The mandibular symphysis is short, and its external surface is slightly convex and dorsoventrally high (MOZ 6140P; fig. S2). A broad and deep sulcus extends on the lateral surface of the dentaries and surangular, ending in a large foramen at both ends (as in *D. maximus*). The external mandibular fenestra is completely obliterated.

The upper dentition is composed of 3 premaxillary and 10 (or 11) large maxillary teeth, which is an unusually low number of teeth for a marine crocodyliform. Most thalattosuchians have between 25 and 40 small teeth, except for *D. maximus*, which has a minimum of 20 teeth in the upper tooth row (*2*). All preserved teeth of *D. andiniensis* are large, robust, poorly curved, and interlock extensively with the lower dentition (Fig. 1E). The crowns are lateromedially compressed and have serrated margins, resembling only those of *D. maximus* (*7*) among marine crocodyliforms. The denticles have a proportionately large basal length with respect to their height and are well separated from each other by broad cella and interdenticular slits (Fig. 1, F and G). The profile of the denticles is rounded in buccal view, but the serrations bear a sharp cutting edge on the mesial and distal margins (Fig. 1F). The outer enamel surface of all preserved teeth is divided into a basal smooth zone and a wrinkled apical region, with distinct, ring-like depressions.

This dental morphology is unique among marine reptiles; only some mosasaurs have serrated teeth, but they have remarkably small denticles (*12*). In contrast, the presence of denticles is common among terrestrial carnivorous archosaurs, including some crocodyliforms [e.g., *Baurusuchus*, *Iberosuchus*, *Sebecus*, and *Pristichampsus* (*1*, *9*, *13*, *14*)]. However, the serrated teeth of terrestrial crocodyliforms are chisel-shaped, with a shorter basal length, larger diaphyseal height, and narrow interdenticular slits (*12*, *14*–*16*). These differences are consistent with the independent origin of ziphodont dentition in *Dakosaurus* inferred from the phylogenetic results.

A phylogenetic data set was gathered considering representatives of all major clades of Crocodyliformes (*17*, *18*). The cladistic analysis places *D. andiniensis* as closely related to *D. maximus* (Fig. 2), as indicated by the presence of a proportionately higher rostrum and lateromedially compressed and serrated teeth. This group is deeply nested within Metriorhynchidae, the clade of crocodyliforms with the most remarkable adaptations to the marine environment [e.g., paddle-like forelimbs, hypocercal tail, osteoporotic-like bone (*19*), and hypertrophied nasal salt glands (*20*)]. This group is well supported by the data and diagnosed by numerous cranial synapomorphies present in *D. andiniensis* (*17*). The available postcranial material of *D. andiniensis* is too scarce to assess if the swimming capabilities of this crocodyliform were similar to those of other metriorhynchids.

The phylogenetic hypothesis implies that the *Dakosaurus* lineage evolved from the ancestral gracile condition present in most thalattosuchians (Fig. 2). Within this framework, the European *D. maximus* represents an initial stage in the evolution of a lineage that departs from the above-mentioned conditions, showing the acquisition of relatively enlarged teeth with serrated margins and a moderately high snout, but preserving many plesiomorphies of other metriorhynchids (e.g., large number of teeth, elongated symphysis, and snout length occupying more than 60% of the skull). However, the unusual morphology of *D. andiniensis* creates a large morphological gap between this taxon and all other marine crocodyliforms.

One of the most striking differences is the extremely high and robust rostrum in *D. andiniensis*. We considered the variation in rostral height and length through the optimization of their ratio across the phylogenetic tree of Crocodyliformes using the maximum parsimony criterion (Fig. 3). As optimized in the tree, this analysis illustrates the differences between

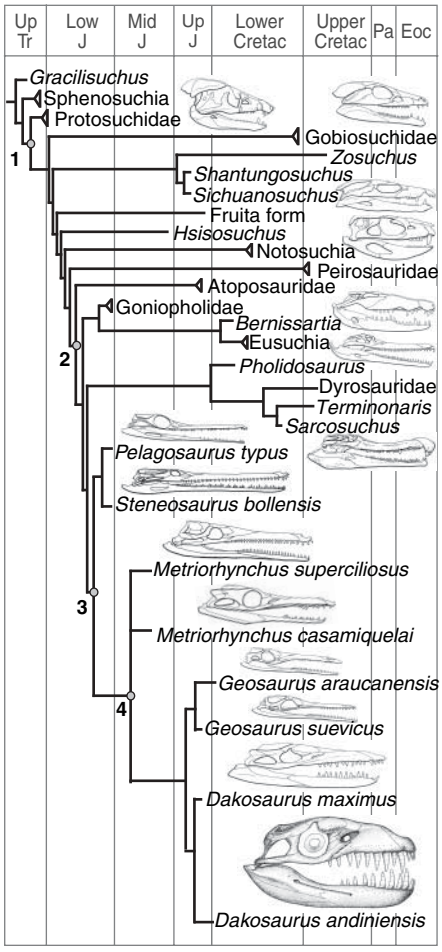

Fig. 2. Phylogenetic relationships of Crocodyliformes obtained in the cladistic analysis, plotted against geochronologic epochs (strict consensus of most parsimonious trees; some taxa distantly related to *D. andiniensis* collapsed into triangular clades). Only skull figures of Thalattosuchia were drawn to the same scale (*17*). Numbered nodes: 1, Crocodyliformes; 2, Neosuchia; 3, Thalattosuchia; and 4, Metriorhynchidae. Further phylogenetic information is available in (*17*).

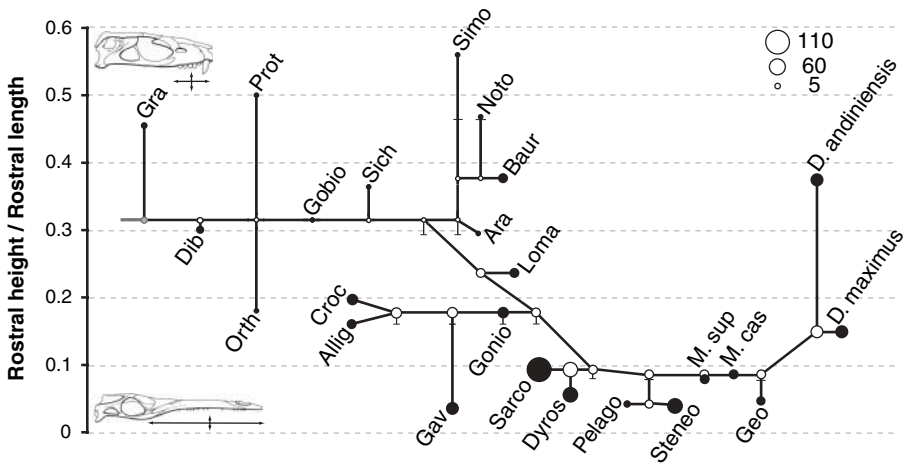

Fig. 3. Phylogenetic tree of Crocodyliformes displaying the evolution of rostral shape, as measured by the rostral height/rostral length ratio optimized using TNT (*28*, *29*). The root of the tree located on the left side of the figure (marked in gray) and derived forms are toward the right. The vertical location of the nodes is determined by the ratio values following the ordinate axis [solid circles, measured species (*17*); empty circles, inferred ancestral values; error bars, ranges of possible ancestral values]. Circle size represents the absolute value of rostral length measured in terminal taxa and inferred for ancestral nodes (scale for circle size and rostral length in cm in top right corner) (*17*). Abbreviations: Gra, *Gracilisuchus*; Dib, *Dibothrosuchus*; Orth, *Orthosuchus*; Prot, *Protosuchus*; Gobio, *Gobiosuchus*; Sich, *Sichuanosuchus*; Simo, *Simosuchus*; Noto, *Notosuchus*; Baur, *Baurusuchus*; Ara, *Araripesuchus*; Loma, *Lomasuchus*; Gonio, *Goniopholis*; Gav, *Gavialis*; Croc, *Crocodylus niloticus*; Allig, *Alligator*; Sarco, *Sarcosuchus*; Dyros, *Dyrosaurus*; Steneo, *Steneosaurus*; Pelago, *Pelagosaurus*; M. sup, *Metriorhynchus superciliosus*; M. cas, *Metriorhynchus casamiquelai*; Geo, *Geosaurus araucanensis*.

D. andiniensis and other marine taxa and reveals the major trends in rostral change along the evolutionary history of Crocodyliformes.

The large diversity of rostral shapes among basal terrestrial crocodyliforms (*21*) is reflected in the disparity of rostral height/length ratios among these small forms (Fig. 3, left). However, this graph shows a clear phylogenetic trend in neosuchian crocodyliforms toward longer rostra that are proportionately low dorsoventrally (Fig. 3, right). These morphological changes coincide with a shift toward the aquatic habits inferred for most neosuchian taxa and have been explained as adaptations to this environment, related changes in feeding strategies, and increases in mechanical resistance in their rostra (*1*, *9*, *22*).

Although different rostral morphologies are present in living crocodylians (*23*) and moderate cases of rostral shortening have been reported in some longirostrine groups (*17*, *24*, *25*), the general trend toward long and low snouts is present in most neosuchian groups (Fig. 3). This trend reaches an extreme condition in thalattosuchian crocodyliforms, depicting the characteristic elongated and gracile snouts of these marine crocodyliforms. The hyperdentate tubular rostrum in this group has long been considered as an adaptation to feeding on small agile prey, such as mollusks (*26*) or fishes [based on the diet of extant crocodylians with similar rostral morphology (e.g., *Gavialis*) (*1*, *9*, *22*)]. The feeding strategy of these taxa is usually inferred to be based on rapid lateral movements, facilitated by the large angular speed and low hydrodynamic resistance of their elongated and low rostra (*1*, *9*, *22*).

The *Dakosaurus* lineage appears to have reversed this trend in a drastic morphological change, with *D. maximus* an incipient representative of this condition and *D. andiniensis* the most extreme case of rostral modification (Fig. 3). The relatively short and high rostrum and ziphodont dentition probably reflects a modified feeding strategy, because the hydrodynamic advantages allowing rapid lateral movements would not be present in *D. andiniensis*. Although the snout height/length ratios depict similar values for *D. andiniensis* and some terrestrial crocodyliforms (e.g., *Baurusuchus*), there are remarkable differences in other aspects of their rostral shape, such as the reduced width of the snout and the vertically orientated maxillae of these terrestrial forms.

References and Notes

1. W. Langston, in *The Biology of Reptilia 4*, C. Gans, T. Parsons, Eds. (Academic Press, New York, 1973), pp. 263–284.
2. P. Vignaud, thesis, Université Poitiers (1995).
3. Z. Gasparini, M. Fernández, in *The Neuquén Basin: a Case Study in Sequence Stratigraphy and Basin Dynamics* (Special Publication 252), G. Veiga, L. Spalletti, E. Schwarz, J. Howell, Eds. (Geological Society of London, London, 2005), pp. 279–294.
4. J. Howell, E. Schwarz, L. Spalletti, G. Veiga, in *The Neuquén Basin: a Case Study in Sequence Stratigraphy and Basin Dynamics* (Special Publication 252), G. Veiga, L. Spalletti, E. Schwarz, J. Howell, Eds. (Geological Society of London, London, 2005), pp. 1–14.
5. L. Spalletti, J. Franzese, S. Matheos, E. Schwarz, *J. Geol. Soc. London* **157**, 433 (2000).
6. P. Vignaud, Z. Gasparini, *C. R. Acad. Sci. Paris* **322**, 245 (1996).
7. E. Fraas, *Palaeontographica* **49**, 1 (1902).
8. *D. andiniensis*, holotype: MHNSR PV34 (Museo de Historia Natural de San Rafael, Mendoza Province, Argentina). Fragment of rostrum composed by parts of the maxilla, nasal, and premaxilla, lacking tooth crowns (*6*). Referred specimens: MOZ 6146P (Museo Profesor J. Olsacher, Zapala, Neuquén Province, Argentina), almost complete skull and lower jaws; MOZ 6140P, lower jaw and fragmentary postcranial elements. See (*17*).
9. A. B. Busbey, in *Functional Morphology in Vertebrate Paleontology*, J. Thomason, Ed. (Cambridge Univ. Press, Cambridge, 1995), pp. 173–192.
10. J. M. Clark, in *In the Shadow of the Dinosaurs: Early Mesozoic Tetrapods*, N. Fraser, H.-D. Sues, Eds. (Cambridge Univ. Press, New York, 1994), pp. 84–97.
11. Z. Gasparini, D. Dellapé, *Actas I Congr. Geol. Chile* **1**, C1 (1976).
12. J. O. Farlow, D. L. Brinkman, W. L. Abler, P. J. Currie, *Mod. Geol.* **16**, 161 (1991).
13. I. S. Carvalho, A. C. Arruda Campos, P. H. Nobre, *Gondw. Res.* **8**, 11 (2004).
14. D. Riff, A. W. Kellner, *Bull. Mus. Nac. Nov. Ser. Geol.* **59**, 1 (2001).
15. G. V. R. Prasad, F. L. de Broin, *Ann. Paleontol.* **88**, 19 (2002).

16. O. Legasa, A. D. Buscalioni, Z. Gasparini, *Stud. Geol. Salm.* **29**, 127 (1994).
17. Materials and methods are available as supporting material on *Science* Online.
18. The phylogenetic data set included 257 characters scored across 58 crocodylomorph taxa at the species level, expanding previously published data sets (*27*), and was analyzed using parsimony in TNT v.1.0 (*28*). See (*17*) for further details.
19. S. Hua, V. de Buffrenil, *J. Vertebr. Paleontol.* **16**, 703 (1996).
20. M. Fernández, Z. Gasparini, *Lethaia* **33**, 269 (2000).
21. G. A. Buckley, C. A. Brochu, D. W. Krause, D. Pol, *Nature* **405**, 941 (2000).
22. N. N. Iordansky, in *The Biology of Reptilia* **4**, C. Gans, T. Parsons, Eds. (Academic Press, New York, 1973), pp. 201–262.
23. C. A. Brochu, *Am. Zool.* **41**, 564 (2001).
24. S. Jouve, B. Bouya, M. Amaghzaz, *Palaeontology* **48**, 359 (2005).
25. M. Delfino, P. Piras, T. Smith, *Acta Palaeontol. Pol.* **50**, 565 (2005).
26. D. M. Martill, *Neues Jahrb. Geol. Palaeontol. Monatsh.* **1986**, 621 (1986).
27. D. Pol, M. A. Norell, *Am. Mus. Novit.* **3458**, 1 (2004).
28. P. A. Goloboff, J. S. Farris, K. Nixon, TNT ver. 1.0. Program and documentation available from the authors and at www.zmuc.dk/public/phylogeny (2003).
29. P. A. Goloboff, C. I. Mattoni, A. S. Quinteros, *Cladistics* **20**, 595 (2004).
30. The specimens reported here were found by S. Cocca and R. Cocca from the Museo Olsacher (Dirección de Minería, Neuquén Province, Argentina) and prepared by J. Moly (Museo de La Plata). Scanning electron microscope images were taken by R. Urréjola. Drawings for Figs. 1 to 3 were executed by Jorge González. We thank S. Jouve, S. Hwang, and G. Erickson for discussions, and we acknowledge the support of Museo Olsacher, the Dirección de Minería, and Secretaría de Cultura (Neuquén Province). This project was funded by the National Geographic Society (to Z.G.), Agencia Nacional de Promoción Científica y Tecnológica (to Z.G. and L.A.S.). Part of the phylogenetic study was conducted with the support of the American Museum of Natural History (to D.P.).

Supporting Online Material

www.sciencemag.org/cgi/content/full/1120803/DC1
Materials and Methods
Figs. S1 and S2
References

30 September 2005; accepted 1 November 2005
Published online 10 November 2005;
10.1126/science.1120803
Include this information when citing this paper.

The Late Miocene Radiation of Modern Felidae: A Genetic Assessment

Warren E. Johnson,[1]* Eduardo Eizirik,[1,2] Jill Pecon-Slattery,[1] William J. Murphy,[1]† Agostinho Antunes,[1,3] Emma Teeling,[1]‡ Stephen J. O'Brien[1]*

Modern felid species descend from relatively recent (<11 million years ago) divergence and speciation events that produced successful predatory carnivores worldwide but that have confounded taxonomic classifications. A highly resolved molecular phylogeny with divergence dates for all living cat species, derived from autosomal, X-linked, Y-linked, and mitochondrial gene segments (22,789 base pairs) and 16 fossil calibrations define eight principal lineages produced through at least 10 intercontinental migrations facilitated by sea-level fluctuations. A ghost lineage analysis indicates that available felid fossils underestimate (i.e., unrepresented basal branch length) first occurrence by an average of 76%, revealing a low representation of felid lineages in paleontological remains. The phylogenetic performance of distinct gene classes showed that Y-chromosome segments are appreciably more informative than mitochondrial DNA, X-linked, or autosomal genes in resolving the rapid Felidae species radiation.

The first felidlike carnivores appeared in the Oligocene, approximately 35 million years ago (Ma). Living cat species (subfamily Felinae) originated in the late Miocene and evolved into one of the world's most successful carnivore families, inhabiting all the continents except Antarctica (*1*, *2*). Understanding their evolutionary history and establishing a consensus taxonomic nomenclature has been complicated by rapid and very recent speciation events, few distinguishing dental and skeletal characteristics, incidents of parallel evolution, and an incomplete fossil record (*1*–*5*). Recent analyses (*6*–*8*) identified eight major felid lineages, although their chronology, branching order, and exact composition remained unresolved (*4*–*8*). Here, we present an analysis of DNA sequence from 19 independent autosomal (aDNA), five X-linked (xDNA), six Y-linked (yDNA), and nine mitochondrial (mtDNA) gene segments (tables S1 to S3) sampled across the 37 living felid species plus 7 outgroup species representing each feliform carnivoran family (*9*).

We present a phylogenetic analysis (Fig. 1) for nuclear genes (nDNA) [combined y, x, and aDNA = 18,853 base pairs (bp)] that leads to several conclusions. First, the eight Felidae lineages are strongly supported by bootstrap analyses and Bayesian posterior probabilities (BPP) for the nDNA data and most of the other separate gene partitions (Table 1 and figs. S1 to S11), by rare shared derived indels, including endogenous retroviral families in the domestic cat lineage (*10*), by transposed nuclear mtDNA sequences (*Numt*) in the domestic cat (node 9) and *Panthera* lineages (node 33) (*11*, *12*) (Table 1 and table S7), by 11 to 65 diagnostic sites for individual lineages (tables S5 and S8), and by amino acid data analyses of 14 genes (1457 sites) (tables S9 and S10 and fig. S1). Second, the four species previously unassigned to any lineage (marbled cat, serval, pallas cat, and rusty spotted cat) (*6*) have now been confidently placed. Third, the hierarchy and timing of divergences among the eight lineages are clarified (Fig. 1 and Table 1). Fourth, the phylogenetic relationships among the nonfelid species of hyenas, mongoose, civets, and linsang corroborate previous inferences with strong support (*13*, *14*).

The radiation of modern felids began with the divergence of the *Panthera* lineage leading to the clouded leopard and the "great roaring cats" of the *Panthera* genus (node 33 in Fig. 1). Support for this basal position was strong (88 to 100%) with all analytic methods and gene partitions (Table 1 and table S4) contrasting with some previous results that suggested a more internal position for the big cats (*7*). The split of the *Panthera* lineage was followed by a rapid progression of divergence events. The first led to the bay cat lineage, a modern assemblage of three Asian species (bay cat, marbled cat, and Asian golden cat) (node 31), followed by divergences of the caracal lineage, with three modern African species (caracal, serval, and African golden cat) (node 29) and of the ocelot lineage (node 23), consisting of seven Neotropical species. Bootstrap support (BS) for the nodes that produced these three early divergences (nodes 2 to 4) was moderate (74 to 97% nDNA BS) relative to nodes defining lineage groups (23, 29, and 31) with 100% nDNA BS. A more recent clade, including four lineages (lynx, puma, leopard cat, and domestic cat lineages) (node 5), is well supported (97 to 99% nDNA BS). The divergence of the lynx lineage was followed very closely by the appearance of the puma lineage (Fig. 1). However, these two North American groups were united as sister groups in some analyses using different data partitions and phylogenetic algorithms (figs. S6 to S11 and

[1]Laboratory of Genomic Diversity, National Cancer Institute, Frederick, MD 21702–1201, USA. [2]Centro de Biologia Genômica e Molecular, Faculdade de Biociências, Pontifícia Universidade Católica do Rio Grande do Sul, Avenida Ipiranga 6681, Porto Alegre, RS 90619-900, Brazil. [3]REQUIMTE, Departamento de Química, Faculdade de Ciências, Universidade do Porto, Rua do Campo Alegre, 687, 4169-007 Porto, Portugal.

*To whom correspondence should be addressed. E-mail: johnsonw@ncifcrf.gov (W.E.J.); obrien@ncifcrf.gov (S.J.O.)
†Present address: Department of Veterinary Integrative Biosciences, Texas A&M University, College Station, TX, 77843–4458, USA.
‡Present address: Department of Zoology, University College Dublin, Belfield, Dublin 4, Ireland.